Topological reponse theory for flow networks

Dirk Witthaut
(Dated: February 5, 2015)

We analyze the response of a flow network to local damages or link failures. Using a dual representation in terms of cycle flows, we can predict the change of networks flows in an intuitive way using only on the topology of the network. As an example we show that the effect of transmission line failures in power grids can be understood from purely topological features of the network.

I. INTRODUCTION

Transportation, or flow networks are a key concept in the modeling of many natural as well as man made complex systems. Important examples include power grids (flow of energy), river basins (flow of water on a grand scale), or the vascular network of mammals and plants (flow of blood and water, respectively). In order to maintain their functionality, many such systems need to be designed to be robust against damage. This task can be taken over either by humans (power grids) or evolution through natural selection (vascular networks). However, because of the complex nature of many flow networks, predicting the effects of a perturbation can be challenging, as they depend strongly on the precise details such as position of the damaged edge. Therefore, investigating the effects of perturbations in complex flow networks is an important endeavour, not only to improve the design of man made systems, but also to further our understanding of evolutionary processes.

In this work we study the linearized effect of perturbations in planar networks which can be used to describe e.g. the venation network in vascular plant leaves, which is naturally planar, or power grids, which can be taken to be planar to a good approximation. We take a point of view dual to previous work, expressing the effect of a small perturbation in terms of cycle currents on the fundamental cycles (facets) of the networks. We show that a small perturbation induces two domains of oppositely oriented cycle currents on the network whose strength decays with shortest path distance on the dual graph and provide an algorithm that uses network topology to predict the direction of flow change due to the perturbation. We then proceed to apply our theory to two important test cases. First, we consider the linear flow network in one leaf of Norway maple (*Acer platanoides*) which was chemically cleared, scanned and had its network vectorized. We show that in this case, decay of the cycle currents is exponential. Second, we apply our method to the prediction of blackouts in nonlinear power grids, comparing the topologically predicted direction of flow change with numerically exact simulations, finding perfect agreement.

II. THE CONTINUITY EQUATION AND ITS DUAL REPRESENTATION

The *continuity equation* is the fundamental relation describing the steady state of a flow network: The sum of all flows to or from a node j must equal the source or sink strength P_j:

$$\sum_{\ell=1}^{N} F_{j\ell} = P_j \,. \tag{1}$$

In many important applications the flow is proportional to the potential drop along the edge. More general, we consider networks, where the flow is given by

$$F_{j\ell} = K_{j\ell} f(\phi_\ell - \phi_j) \tag{2}$$

with an antisymmetric function $f(\cdot)$ and the transport capacity or conductivity $K_{j\ell} = K_{\ell j}$. The steady state of the network is then determined by the equations

$$\sum_{\ell=1}^{N} K_{j\ell} f(\phi_\ell - \phi_j) = P_j \,. \tag{3}$$

for all $j = 1, \ldots, N$ nodes of the network. This holds for DC electric circuits ('Kirchhoffs' law'), hydraulic networks [**?**] or vascular networks of plants [**?**]. AC power grids, which form the basis of our technical infrastructure, are discussed in more detail in section VI. Equation (3) also describes the steady state of oscillator networks such as the celebrated Kuramoto model [**? ? ?**], where ϕ_j is a phase variable.

An important question in network operation is the resilience to local damages: How does the network respond when the capacity of a single edge $K_{j\ell}$ is reduced or vanishes entirely? Is it stable or does the local failure induce a global blackout? Here we introduce a geometric theory of flow re-distribution after local damages based on the *dual representation* of the network flow problem. To this end we introduce the edge incidence matrix $E \in \mathbb{R}^{N\times L}$, L being the total number of edges [**?**]. The elements of the matrix are $E_{j,e} = 1$ if the node j is the head of the edge e, $E_{j,e} = -1$ if j is the tail of e and $E_{j,e} = 0$ otherwise. For the calculations we have to choose an orientation of the edges, which is arbitrary but must kept fixed. The continuity equation (1) then reads

$$\sum_{e=1}^{L} E_{j,e} F_e = P_j \tag{4}$$

This is an underdetermined equation for the flows, whose solutions span an $(L-N+1)$-dimensional affine subspace. The homogeneous solutions correspond to *cycle flows* in the network, which do not affect the flow balance at the nodes.

Lemma 1. *All solutions to the continuity equation can be expressed as*

$$F_e = F_e^{(0)} + \sum_{c=1}^{L-N+1} f_c C_{c,e}, \qquad f_c \in \mathbb{R}, \tag{5}$$

where $F_e^{(0)}$ is one special solution of the inhomogeneous equation.

If the flows are given by equation (2), we must further assure that the potentials or phases ϕ_j are unique. This condition is satisfied if the potential differences $\phi_j - \phi_i$ summed around each basis cycle of the network add up to zero (modulo 2π if ϕ_j is a phase variable). If the function f is invertible, this condition can be written in terms of the flows as

$$\sum_{e=1}^{L} C_{c,e} f^{-1}(F_e/K_e) = 0. \tag{6}$$

The coupling function f must be strictly monotonic to be be invertible. For the sake of definiteness we assume that f is strictly monotonically increasing w.l.o.g. This is automatically satisfied for a potential flow where f is just the identity. If we are dealing with phase variables and a sinusoidal coupling function, we must demand that all phase difference are in the interval $(-\pi/2, +\pi/2)$. Notably, this guarantees the dynamic stability of an oscillator network [**?**].

Now we consider the case that that the capacity of a single edge e_0 is slightly perturbed, $K'_{e_0} = K_{e_0} + \kappa$. To restore the phase condition (6) without affecting the continuity equation (4), we must add a suitable amount of cycle flows to the network. To calculate the perturbed solution explicitly, we choose the flows in the unperturbed network as the special solution $F_e^{(0)}$ in the decomposition (5). Expanding equation (6) to leading order in κ then yields a linear set of equations for the induced cycle flows

$$\sum_{c=1}^{L-N+1} A_{d,c} f_c = \kappa q_d. \tag{7}$$

The matrix A is given by

$$A_{d,c} = \sum_{e=1}^{L} C_{d,e} C_{c,e}\, g(F_e^{(0)}/K_e), \tag{8}$$

where g denotes the derivative of the inverse of the coupling function, $g = (f^{-1})'$. The inhomogeneity

$$q_d = C_{d,e_0}\, g(F_{e_0}^{(0)}/K_{e_0}) F_{e_0}^{(0)}/K_{e_0} \tag{9}$$

is non-zero only for the two cycles adjacent to edge e_0. Calling these two cycles c_1 and c_2, we have $q_{c_1} = -q_{c_2}$. If the edge e_0 lies on the boundary of the network, only one element is non-zero.

III. TOPOLOGY OF CYCLE FLOWS

Equation (7) determines the linear response of the network to local perturbations. The formulation directly yields the flows F_e instead of the potentials ϕ_j. This allows for an intuitive geometric understanding especially for planar graphs, which includes many important natural and man-made supply networks. In this case the fundamental cycles are simply given by the faces of the network, which form the so-called *dual graph* [**?**]. In particular, we obtain the following result for the cycle flows using only the topology of a planar network.

Proposition 1. *A perturbation of the capacity K_{e_0} of a single edge e_0 in a supply network induces cycles flows f_c which are to leading order given by equation (7). If the network is planar, then the dual graph can be decomposed into exactly two connected subgraphs ('domains') $\mathcal{D}_+$ and $\mathcal{D}_-$, with $f_c \geq 0\, \forall c \in \mathcal{D}_+$ and $f_c \leq 0\, \forall c \in \mathcal{D}_-$. The domain boundary includes the perturbed edge e_0, i.e. the two cycles adjacent to e_0 belong to different domains.*

A proof is given in appendix A. The implications of the proposition are illustrated in figure 1 (c), showing the induced cycle flows when the dashed edge is damaged such that its transmission capacity decreases. The cycle flows are positive in one domain and negative in the other domain. If the perturbed edge lies on the boundary of a finite network, then there is only one domain and all cycle flows are oriented in the same direction.

With this result we can obtain a purely geometric prediction of how the flow of all edges in the network change after the perturbation. For this, we need some additional information about the magnitude of the cycle flows in addition to the signs. We consider the upper and lower bound for the cycle flows f_c at a given distance to the cycle c_1 with $\kappa q_{c_1} > 0$ and the cycles c_2 with $\kappa q_{c_2} > 0$, respectively:

$$\begin{aligned} u_d &= \max_{c,\mathrm{dist}(c,c_1)=d} f_c \\ \ell_d &= \min_{c,\mathrm{dist}(c,c_2)=d} f_c. \end{aligned} \tag{10}$$

Proposition 2. *The maximum (minimum) value of the cycle flows decreases (increases) monotonically with the distance to the reference cycles c_1 and c_2, respectively:*

$$\begin{aligned} u_d &\leq u_{d-1}, \qquad 1 \leq d \leq d_{\max}. \\ \ell_d &\geq \ell_{d-1}, \qquad 1 \leq d \leq d_{\max}. \end{aligned} \tag{11}$$

A proof is given in appendix B. Strict monotonicity can be proven when some additional technical assumptions are satisfied, which is expected to hold in most cases. In fact, one finds that the decay is rather fast for many networks of interest:

(1) For two-dimensional lattices with regular topology and edge weights the cycle flows decay with the inverse

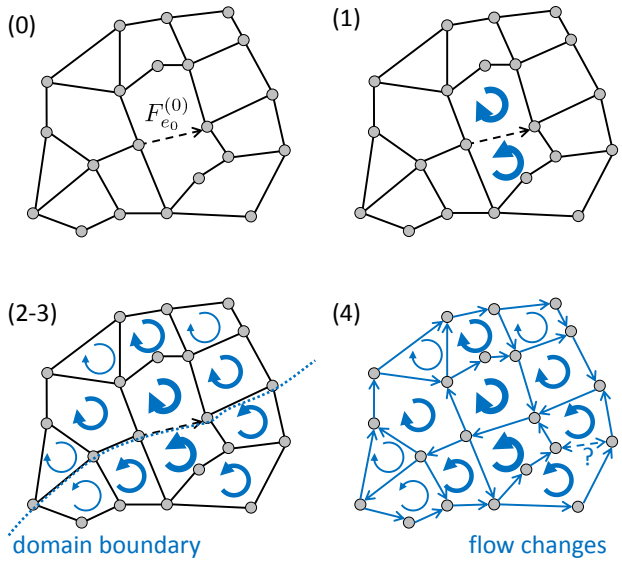

FIG. 1. Schematic representation of the algorithm 1 to predict flow changes after the damage of a single edge (dashed).

distance. A proof for square lattices in the continuum limit is given in appendix C.

(2) For two-dimensional lattices with regular topology but disordered edge weights, the eigenstates of A generally decay exponentially with the euclidean distance. This statement is a manifestation of Anderson localization and was confirmed numerically for many random network ensembles [**XXX references XXX**]. [**?**].

These results imply that the cycle flows $|f_c|$ decay rather rapidly with the distance such that the reponse of a supply network is confined to the 'vicinity' of the damaged edge. However, it has to be noted that the distance is defined for the dual graph, not the original graph, and that the rigoros results hold only for planar graphs. The situation is much more involved in non-planar graphs, as an edge can link regions which would be far apart otherwise.

We are thus in the position to predict the change of network flows on a purely topological basis according to the following algorithm whose steps are illustrated in figure 1.

Algorithm 1. *(Prediction of flow changes)*

1. *Assign a cycle flow to the cycles directly adjacent to the perturbed edge e_0, denoted by c_1 and c_2 in the following. If $\kappa < 0$, these cycle flows are anti-parallel to $F^{(0)}_{e_0}$, if $\kappa > 0$ the cycle flows are parallel to $F^{(0)}_{e_0}$.*

2. *Assign a cycle flow with the same orientation to all cycles adjacent to c_1 and c_2. If a cycle is adjacent to both c_1 and c_2, the flow direction for this cycle cannot be decided. Assume that the strength of the cycle flow is weaker.*

3. *Repeat this for the next-to-nearest neighbors and so on.*

4. *The direction of flow change of each edge is then given by the direction of the strongest cycle flow in the two adjacent cycles. The flow over a bridge and the flows in disconnected cycles remain unchanged.*

IV. LINEAR FLOW IN PLANAR GRAPHS

In case of linear flow, i.e. where the flow across an edge is linearly proportional to the potential difference across it, lends itself to easier analysis because (8) simplifies to

$$A_{d,c} = \sum_{e=1}^{L} C_{d,e} C_{c,e} \tag{12}$$

$$= \begin{cases} \text{Number of edges shared by faces c and d} & \text{if } c \neq d \\ \text{Number of edges in face c} & \text{if } c = d \end{cases} \tag{13}$$

Then the matrix A can be seen as a part of the Laplacian of the dual Graph of G, the original network.

Let L be a full Laplacian of the dual graph $D(G)$, whose 1st row corresponds to the *unbounded face* of G. Then A can be simply obtained by deleting the first row and first column of L.

$$L = \left(\begin{array}{c|ccc} L_{11} & L_{12} & L_{13} & \cdots \\ \hline L_{21} & & & \\ L_{31} & & A & \\ L_{41} & & & \end{array}\right)$$

Since the laplacian of a graph is closely connected to the resistance distance [**?**], we can obtain the relationship

$$f_c \propto R_{c,c_1} - R_{c,c_2} \tag{14}$$

(for derivation see Appendix D).

Now we discuss how the decay of cycle flow differs in different network topologies.

A. Square lattice

We have computed the cycleflows in a 200×200 square lattice, when the link between the nodes $(0,0)$ and $(0,1)$ is perturbed. The results are shown in figure 2, where we show how the cycleflows f_c decay with distance from the source of perturbation. We see that cycle flow is inversely proportional to the distance from the source of the perturbation, when the distance is small compared to the lattice size. However, the decay is much more rapid near the edge of the lattice.

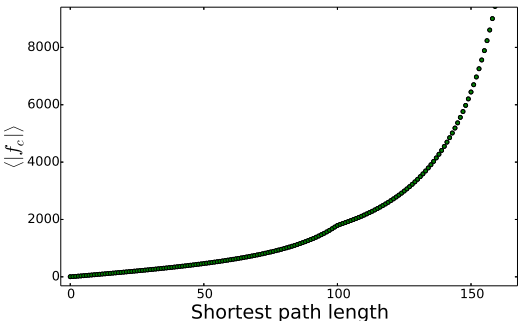

FIG. 2. Decay of cycle for in a square lattice of size 200x200

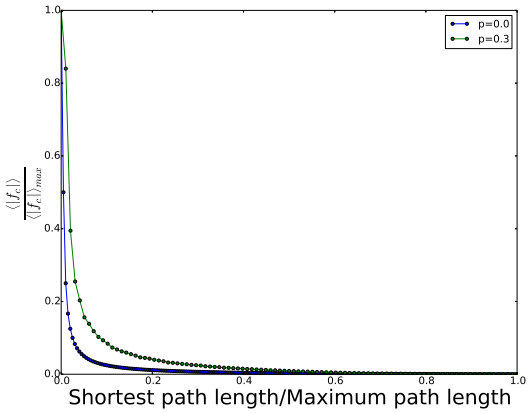

FIG. 3. Decay of cycle for in a square lattice with randomness factor p

B. Effect of randomness in the lattice

Now we observe the effect of introducing randomness in the square lattice. For each node, we merged it with one of its randomly chosen neighbours with small probability p. As we see in figure 3, the introduction of randomness slows down the decay of cycle flows.

However, as we see in figure 4, there still exists a region extending from the source of the perturbation till 40% of the diameter of the graph where the decay of cycle flow is linear.

V. VASCULAR NETWORKS

Vascular plants possess an intricate, highly reticulate network supplying the leaf blade with water for gas exchange through evaporation as well as photosynthesis. The transport of water in these vascular networks can be described by a potential flow as shown in [**?**]. As leaf networks are naturally planar, our theorem can be used to predict the direction of flow changes after a damage to the leaf.

We demonstrate this by simulating the cycle flow arising from perturbing the main vein of one leaf of Norway maple (*Acer platanoides*). The leaf was chemically cleared and stained to make the complete network visible, then scanned at high resolution (3200 dpi) and the vascular network extracted using a vectorization approach. The result is a complete representation of the network topology and geometry.

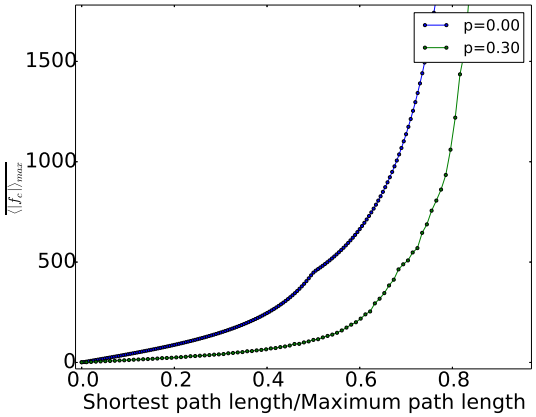

FIG. 4. Inverse of f_c for in a square lattice with randomness factor p

Flow through an edge is described by $F_e = k\frac{R_e^4}{L_e}(p_{e_0} - p_{e_1}$, where R_e is edge radius, L_e is edge length, p_{e_i} is hydrostatic pressure at node e_i, and k is a constant of proportionality. This is basically Poiseuille's law.[**?**] The continuity equation is $\sum_e E_{i,e}F_e = P(1 + (N-2)\delta_{i,0})$, modeling uniform evaporation of water over the whole leaf blade except at the petiole ($i = 0$), which acts as an inlet.

Since the flow equation is linear in the pressure difference, the flow change due to the perturbation is indeed exactly (up to a constant factor) described by equation (7). The simulation results are shown in figure 5. It is interesting to note that (a) the domain boundary between cycle flows of opposite orientation follows the leaf symmetry axis (the main vein) almost exactly. When perturbing other veins, the domain boundary similarly appears to follow the locally thickest veins. Additionally, (b) cycle flow strength on either sides of thick veins appears to jump when there is no domain boundary, effectively confining the perturbation to a localized region. A different localization behavior (c) can be observed by plotting maximum and minimum cycle flow as a function of shortest path distance on the dual graph. Approximately exponential decay is clearly discernible over large distances. The leaf network is thus disordered enough to show Anderson localization of the perturbation. We speculate that this may be functionally relevant for the plant, as damage in one part of the leaf has only local effects, leaving most of the rest functioning undisturbedly.

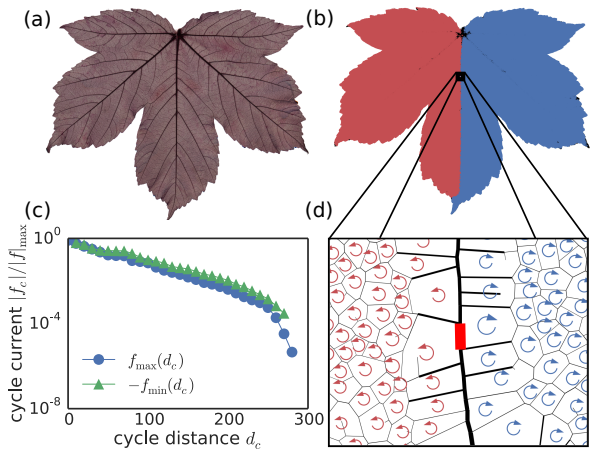

FIG. 5. (a) A leaf blade of Norway maple (*Acer platanoides*), high resolution scan (3200 dpi). The complete venation network up to all orders was extracted from this image. (b) The flow network as extracted from the high resolution scan. One edge on the main vein has been perturbed (approximate position shown by black rectangle), oppositely oriented cycle flows are marked in red and blue. The domain boundary clearly follows the main vein almost perfectly. (c) A semi-logarithmic plot of the absolute value of maximum (blue circles) and minimum (green triangles) cycle flow strength as a function of shortest path distance on the dual graph d_c from the perturbation. Formally, $f_{\max}(d_c) = \max_{d(c',c_{e_0})=d_c} f_{c'}$, where c_{e_0} is one of the cycles adjacent to the perturbed edge e_0 and $d(c,c')$ is the shortest path distance between cycles c and c' in the dual network. The definition of $f_{\min}$ is similar. Solid lines act as a guide for the eye. Decay is approximately exponential, showing strong localization of the perturbation, compatible with results from Anderson localization. (d) Zoom to the region close to the perturbation. The perturbed edge is marked in bright red, oppositely oriented cycle currents are represented by oriented arrows. Arrow size is proportional to cycle flow magnitude, edge diameters are proportional to measured vein diameters but have been downscaled to improve clarity of the image.

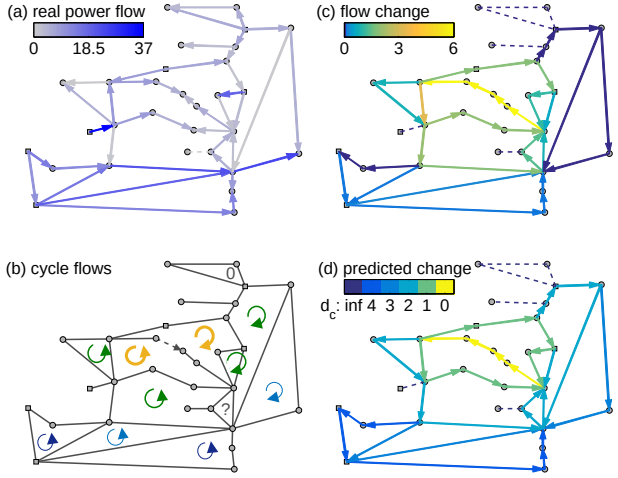

FIG. 6. Predicting flow changes after a transmission line failure in a model power grid. (a) Real power flows in the initial intact network. (b) The failure of a transmission line (dashed) must be compensated by cycle flows indicated by cyclic arrows. The thickness of the lines indicates the strength of the cycle flows. (c) The resulting flow changes after the failure of the marked transmission line. (d) The direction of the flow changes are exactly predicted by algorithm 1 for all edges and the magnitude decreases with the cycle distance d_c. The power flow in (a,c) has been calculated using the standard software MATPOWER for the 30-bus test case [**?**].

VI. PREDICTING BLACKOUTS IN POWER GRIDS

Power grids form the backbone of our technical infrastructure. Their stable operation is essential for our economy and everyday life. Generally, power grids must be operated such that they are resilient against the damage of a single transmission line (the so-called $n-1$ criterion [**?**]). Still, local failures repeatedly induce global outages in periods of extreme loads [**?** **?**], which are expected to become much more likely in the future [**?**]. Any fundamental result that predicts the effects of local failures is thus of great scientific as well as economic value.

Consider an AC electric power grid with N_g generator nodes and N_l load nodes. The continuity equation for the real power reads [**?**]

$$P_k = \sum_{m=1}^{N_g+N_l} U_k U_m \left(G_{km}\cos\phi_{km} + B_{km}\sin\phi_{km}\right), \quad (15)$$

where P_k is the power generation or demand at node k, $U_k e^{i\phi_k}$ is the complex voltage and $\phi_{km} = \phi_k - \phi_m$ abbreviates the phase difference. The coupling of the nodes is described by the nodal admittance matrix $Y_{km} = G_{km} + iB_{km}$. If all votages are constant and ohmic losses can be neglected ($G_{km} = 0$), then we recover the continuity equation in the form discussed in section II,

$$P_k = \sum_{m=1}^{N_g+N_l} U_k U_m B_{km}\sin(\phi_k - \phi_m). \quad (16)$$

These approximations are mostly satisfied in modern power grids. Even more, a linearization as in equation (7) is appropriate when the grid is not too heavily loaded, which yields the so-called DC approximation [**?**]. Most power grids are approximately planar, crossings of transmission lines are possible but rare. We thus expect that the algorithm 1 can still predict the effects of the damage of single transmission lines in real power grids with great accuracy.

We test the algorithm for the 30 bus test grid from [**?**] using both the full AC load flow calculations including ohmic losses and the DC approximation. In the AC case, the voltage U_k of the consumer nodes are free variables

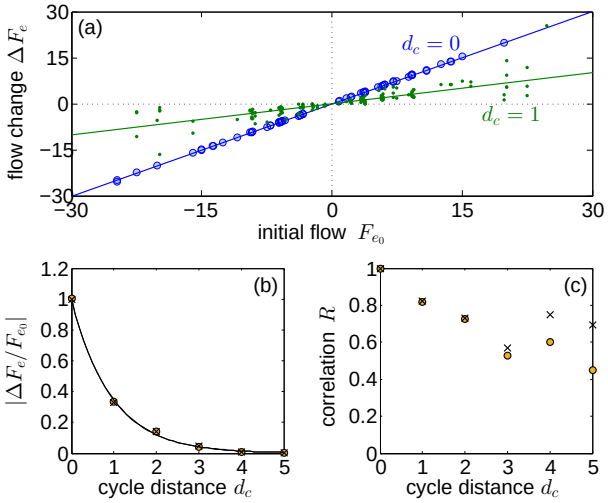

FIG. 7. XXX

whereas the reactive power demand is fixed which yields the additional constraint [**?**]

$$Q_k = \sum_{\ell=1}^{N_g+N_l} U_k U_m \left(G_{km} \sin\phi_{km} - B_{km} \cos\phi_{km}\right). \quad (17)$$

In total, we have $2N_g + N_l$ free variables (N_l voltages and $N_g + N_l$ phase angles) to satisfy the $2N_g + N_l$ nonlinear equations (15) and (17). Figure 6 compares numerically exact values for the real power flows and the flow changes with the topological predictions using algorithm 1. The direction of the flow changes is correctly predicted for all edges. Notably, the flow changes are zero for one disconnected cycle in the north and several bridges.

XXX Discuss figure 7 XXX

XXX Dirk will revise this section and include an example of critical link prediction. XXX

VII. DISCUSSION

XXX TODO XXX

ACKNOWLEDGMENTS

We gratefully acknowledge support from the Helmholtz Association (grant no. VH-NG-1025) and the Federal Ministry of Education and Research (BMBF grant no. 03SF0472E). The work of HR is supported by the IMPRS Physics of Biological and Complex Systems, Göttingen. We wish to thank Torsten Eckstein for providing the cleared maple leaf, and Jana Lasser for contributing vectorization code.

Appendix A: Proof of proposition 1

In the following we analyze the solution of equation (7). W.l.o.g. we assume that both the original network and the dual graph are connected. Otherwise we can just focus on the connected component which includes the perturbed edge resp. the perturbed cycles and exclude all disconnected parts from our analysis.

Definition 1. *A positive domain $\mathcal{D}_+$ is a connected subgraph of the dual with $f_c \geq 0$ for all $c \in \mathcal{D}_+$ and at least one cycle with $f_c > 0$. The domain $\mathcal{D}_+$ is called isolated if $f_d \leq 0$ for all cycles d in the immediate neighborhood of the domain $\mathcal{D}_+$. Analogously we use $\mathcal{D}_-$ for a domain with opposite signs.*

Definition 2. *We denote by $\mathcal{B}$ the set of edges which form the boundary of the graph, i.e. the set of edges which is adjacent to only one cycle in the dual graph:*

$$\mathcal{B} = \left\{ e \in E \middle| \sum\nolimits_c C_{ce} \neq 0 \right\}. \quad (A1)$$

Lemma 2. *Each isolated domain $\mathcal{D}_+$ must contain a cycle c_1 with $q_{c_1} > 0$ and each isolated domain $\mathcal{D}_-$ must contain a cycle c_2 with $q_{c_2} < 0$.*

Proof. To proof this statement assume the opposite: Let $\mathcal{D}'$ be a domain with $f_c \geq 0$ and $\kappa q_c \leq 0$ for all $c \in \mathcal{D}'$ and at least one cycle with $f_c > 0$. Using equation (7) we find that

$$\begin{aligned}\sum_{c\in\mathcal{D}'} A_{cc} f_c &= -\sum_{c\in\mathcal{D}'}\sum_{d\neq c} A_{cd} f_d + \sum_{c\in\mathcal{D}'} \kappa q_c \\ &= -\sum_{c\in\mathcal{D}'}\sum_{\substack{d\in\mathcal{D}'\\ d\neq c}} A_{cd} f_d - \sum_{c\in\mathcal{D}'}\sum_{d\notin\mathcal{D}'} A_{cd} f_d \\ &\quad + \sum_{c\in\mathcal{D}'} \kappa q_c. \end{aligned} \quad (A2)$$

Furthermore, using the definition (8) of the matrix A, we have

$$A_{cc} = -\sum_{d\neq c} A_{dc} + \sum_{e\in\mathcal{B}} C_{ce}^2 g_e \quad (A3)$$

such that

$$\begin{aligned}\sum_{c\in\mathcal{D}'} A_{cc} f_c &= -\sum_{c\in\mathcal{D}'}\sum_{\substack{d\in\mathcal{D}'\\ d\neq c}} A_{cd} f_c - \sum_{c\in\mathcal{D}'}\sum_{d\notin\mathcal{D}'} A_{cd} f_c \\ &\quad + \sum_{c\in\mathcal{D}'}\sum_{e\in\mathcal{B}} C_{ce}^2\, g(F_e^{(0)}/K_e). \end{aligned} \quad (A4)$$

Comparing the two expressions and using the symmetry $A_{cd} = A_{dc}$ we find that

$$\begin{aligned}&-\sum_{c\in\mathcal{D}'}\sum_{d\notin\mathcal{D}'} A_{cd} f_d + \sum_{c\in\mathcal{D}'} \kappa q_c \\ &= -\sum_{c\in\mathcal{D}'}\sum_{d\notin\mathcal{D}'} A_{dc} f_c + \sum_{c\in\mathcal{D}'}\sum_{e\in\mathcal{B}} C_{ce}^2\, g(F_e^{(0)}/K_e). \end{aligned} \quad (A5)$$

This leads to a contradiction as the left-hand side of the equation is smaller or equal to zero, while the right-hand side is larger then zero. Hence, the assumption must be wrong and no such domain $\mathcal{D}'$ exists. □

Corrolary 1. *Consider the solution of equation (7) if exactly one edge e_0 is pertubed or damaged.*

If the edge e_0 lies in the interior of the graph ($e_0 \notin \mathcal{B}$), then we have $\kappa q_{c_1} > 0$ and $\kappa q_{c_2} = -\kappa q_{c_1} < 0$ for the two cycles c_1, c_2 adjacent to the edge e_0 and $q_c = 0$ otherwise. Then c_1 belongs to a domain $\mathcal{D}_+$ and c_2 belongs to a domain $\mathcal{D}_-$ and no further isolated domains can exist.

If the edge e_0 lies on the boundary of the graph ($e_0 \in \mathcal{B}$), then only a single cycle c_1 is affected with $q_{c_1} \neq 0$. Hence there is only one domain in the graph such that $f_c \geq 0$ for all cycles c if $q_{c_1} > 0$ and $f_c \leq 0$ for all cycles c if $q_{c_1} < 0$.

XXX TODO: We have shown that there are at most two isolated domains in this case. It remains to be shown that there are exactly two domains, i.e. that it is impossible to have just one. XXX

Appendix B: Proof of proposition 2

As before we analyze the solution of equation (7) and assume that both the original network and the dual graph are connected. In the following we denote by $\mathrm{dist}(c, c')$ the graph theoretic distance of two vertices c and c' of the dual graph.

Definition 3. *We benote by u_d (ℓ_d) the maximum (minimum) value of cycle flows f_c for all vertices c of the dual graph with a given distance d to a reference vertex c':*

$$\begin{aligned} u_d &= \max_{c,\mathrm{dist}(c,c')=d} f_c \\ \ell_d &= \min_{c,\mathrm{dist}(c,c')=d} f_c. \end{aligned} \tag{B1}$$

Lemma 3. *The maximum value of the cycle flows u_d decreases monotonically with the distance to the reference cycle c_1 for which $\kappa c_1 > 0$:*

$$u_d \leq u_{d-1}, \qquad 1 \leq d \leq d_{\max}. \tag{B2}$$

The minimum ℓ_d increaes monotonically with the distance to the reference cycle c_2 for which $\kappa c_2 < 0$:

$$\ell_d \geq \ell_{d-1}, \qquad 1 \leq d \leq d_{\max}. \tag{B3}$$

Proof. The proof is carried out by induction starting from $d = d_{\max}$. We only give the proof for the maximum, the proof for the minimum proceeds in an analog way.

(1) Base case $d = d_{\max}$: Consider the vertex c of the dual for which $\mathrm{dist}(c, c_1) = d_{\max}$ and f_c assumes its maximum $f_c = u_{d_{\max}}$. Equation (7) yields

$$\begin{aligned} A_{cc} f_c &= -\sum_{b \neq c} A_{cb} f_b \\ &= -\sum_{\substack{b \neq c \\ \mathrm{dist}(b,c_1)=d_{\max}}} A_{cb} f_b + \sum_{\substack{b \neq c \\ \mathrm{dist}(b,c_1)=d_{\max}-1}} A_{cb} f_b. \end{aligned} \tag{B4}$$

We define the abbreviations

$$\mathcal{A}_d = -\sum_{b \neq c, \mathrm{dist}(b,c_1)=d} A_{cb} \tag{B5}$$

and use some important properties of the matrix A:

$$\begin{aligned} &A_{cb} \leq 0 \text{ for } c \neq b \qquad \Rightarrow \qquad \mathcal{A}_d \geq 0 \\ &A_{cc} \geq \mathcal{A}_{d_{\max}} + \mathcal{A}_{d_{\max}-1}\,. \end{aligned} \tag{B6}$$

We can furthermore bound the values of f_b in equation (B4) by $u_{d_{\max}}$ or $u_{d_{\max}-1}$, resepctively, such that we obtain

$$\begin{aligned} u_{d_{\max}} = f_c &\leq \frac{\mathcal{A}_{d_{\max}} u_{d_{\max}} + \mathcal{A}_{d_{\max}-1} u_{d_{\max}-1}}{\mathcal{A}_{d_{\max}} + \mathcal{A}_{d_{\max}-1}} \\ \Rightarrow\ u_{d_{\max}} &\leq u_{d_{\max}-1}, \end{aligned} \tag{B7}$$

(2) Inductive step $d \to d-1$: We consider the vertex c with $\mathrm{dist}(c, c_1) = d$ and $f_c = u_d$. Staring from equation (7) and using the same estimations as above, we obtain

$$\begin{aligned} u_d = f_c &= \frac{\kappa q_c - \sum_b A_{cb} f_b}{A_{cc}} \\ &\leq \frac{\mathcal{A}_{d-1} u_{d-1} + \mathcal{A}_d u_d + \mathcal{A}_{d+1} u_{d+1}}{\mathcal{A}_{d-1} + \mathcal{A}_d + \mathcal{A}_{d+1}}\,. \end{aligned} \tag{B8}$$

Note that the inhomogeneity $\kappa q_c \leq 0$ for all vertices except for $c = c_1$. With the induction hypothesis $u_{d+1} \leq u_d$ this yields

$$\begin{aligned} u_d &\leq \frac{\mathcal{A}_{d-1} u_{d-1} + (\mathcal{A}_d + \mathcal{A}_{d+1}) u_d}{\mathcal{A}_{d-1} + \mathcal{A}_d + \mathcal{A}_{d+1}} \\ \Rightarrow u_d &\leq u_{d-1}. \end{aligned} \tag{B9}$$

which completes the proof. □

Lemma 4. *The maximum (minimum) value of the cycle flows u_d decreases (increases)* strictly *monotonically with the distance to the reference cycle c_1 (c_2)*

$$\begin{aligned} &u_d < u_{d-1}, \\ &\ell_d > \ell_{d-1}, \qquad 1 \leq d \leq d_{\max}. \end{aligned} \tag{B10}$$

if (1) all cycles c at maximum distance from c_1 lie at the boundary of the dual graph,

$$\forall c \text{ with } \mathrm{dist}(c, c_1) = d_{\max}: \tag{B11}$$

$$\exists \text{ edge } e \text{ with } e \in \mathcal{B} \text{ and } C_{ce} \neq 0. \tag{B12}$$

or (2) all extrema u_d and ℓ_d are unique.

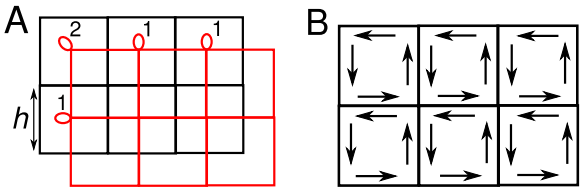

FIG. 8. A. A square lattice (black) together with its cycle-dual (red). The cycle dual is also a square lattice, but because the boundary edges are only adjacent to one cycle, it contains self-loops at its boundary nodes. The weight of a self loop is the sum of all boundary edge weights which are part of the boundary cycle. In the limit $h \to 0$, the self-loops enforce Dirichlet boundary conditions on the cycle density, $\phi|_{\partial A} = 0$. B. Consistently oriented cycles in a square lattice.

Proof. We show that in both cases we can replace $\geq$ by $>$ in the base case and thus also in the inductive step in the proof of lemma 3. If condition (1) is satisfied we have

$$A_{cc} > \mathcal{A}_{d_{\max}} + \mathcal{A}_{d_{\max}-1} \tag{B13}$$

due to boundary terms. If condition (1) is not satisfied but condition (2) is, then the sum in equation B4 includes at least two terms. One of the values of f_b in the sum must be strictly smaller than the maximum value u_d or u_{d-1}, respectively, as we assumed that these maxima are unique. We thus can replace the $\geq$ by $<$ in the estimations.

□

Appendix C: Decay in regular lattices

In this appendix we derive the continuum model directly from the discrete network model in the uniform case. Consider a network with cycle edge adjacency matrix C_{ce}. Then we are interested in a continuous version of equation (**??**). On a square lattice the application of A_{cd} to a vector in the bulk can be written, going to the continuous limit (see Fig. 8),

$$(A\phi)(x) = \frac{\phi(x,y)}{K(x+h/2,y)} + \frac{\phi(x,y)}{K(x-h/2,y)} \tag{C1}$$

$$+ \frac{\phi(x,y)}{K(x,y+h/2)} + \frac{\phi(x,y)}{K(x,y-h/2)} \tag{C2}$$

$$- \frac{\phi(x+h,y)}{K(x+h/2,y)} - \frac{\phi(x-h,y)}{K(x-h/2,y)} \tag{C3}$$

$$- \frac{\phi(x,y+h)}{K(x,y+h/2)} - \frac{\phi(x,y-h)}{K(x,y-h/2)} \tag{C4}$$

$$= h^2 \nabla \cdot \left(\frac{1}{K} \nabla \phi \right) + O(h^3). \tag{C5}$$

Here, h is the lattice spacing. The right hand side works similarly, noting that only two cycles contribute, with opposite signs. Let us assume that e_0 is parallel to the y axis. Then the RHS is

$$- v_y(x+h/2,y) \frac{\kappa}{K(x+h/2,y)(K(x+h/2,y)-\kappa)} \tag{C6}$$

$$\times \delta^{(2)}(x+h/2,y) \tag{C7}$$

$$+ v_y(x-h/2,y) \frac{\kappa}{K(x-h/2,y)(K(x-h/2,y)-\kappa)} \tag{C8}$$

$$\times \delta^{(2)}(x-h/2,y) \tag{C9}$$

$$= h \frac{\partial}{\partial x} \left(v_y \frac{\kappa}{K(K-\kappa)} \delta^{(2)}(x,y) \right) + O(h^3). \tag{C10}$$

This is a dipole source field with dipole moment parallel to the x axis. It is easy to see the generalization to arbitrary dipole moments. Thus, the full continuous equations governing the behaviour of the cycle density in the bulk are

$$\nabla \cdot \left(\frac{1}{K} \nabla \phi \right) = -\boldsymbol{p} \cdot \nabla \delta^{(2)}(\boldsymbol{x} - \boldsymbol{a}), \tag{C11}$$

for a perturbation at $\boldsymbol{a}$. The dipole vector $\boldsymbol{p}$ is orthogonal in direction to flow at the site of perturbation and proportional in magnitude. More perturbations can be handled by linear combination. Note that we have subsumed the factors of h into the derivative by a change of variables $\boldsymbol{x} \to h\boldsymbol{x}$.

At the boundary, a similar relation as in the bulk holds, supplying us with boundary conditions. Because boundary cycles possess three neighboring cycles four edges in total, some terms are left over;

$$(A\phi)(x) = \frac{\phi(x,y)}{K(x+h/2,y)} + \frac{\phi(x,y)}{K(x-h/2,y)} \tag{C12}$$

$$+ \frac{\phi(x,y)}{K(x,y+h/2)} + \frac{\phi(x,y)}{K(x,y-h/2)} \tag{C13}$$

$$- \frac{\phi(x+h,y)}{K(x+h/2,y)} - \frac{\phi(x-h,y)}{K(x-h/2,y)} \tag{C14}$$

$$- \frac{\phi(x,y-h)}{K(x,y-h/2)} \tag{C15}$$

$$= \frac{\phi(x,y)}{K(x,y)} + O(h). \tag{C16}$$

Thus, we find that Dirichlet boundary conditions must hold in the absence of boundary perturbations: $\phi|_{\partial A} = 0$.

Finally, we need a law telling us how to calculate a flow vector from the cycle density. To this end, consider Figure 8 B. In order to obtain the y component of a flow vector, we need to add up the contributions of two cycle flows neighboring in the x direction, and vice versa. Thus, the flow vector becomes

$$\boldsymbol{v}(\boldsymbol{x}) = \begin{pmatrix} \phi(x,y+h/2) - \phi(x,y-h/2) \\ \phi(x-h/2,y) - \phi(x+h/2,y) \end{pmatrix} \tag{C17}$$

$$= \begin{pmatrix} 0 & 1 \\ -1 & 0 \end{pmatrix} \nabla\phi + O(h), \tag{C18}$$

where we again rescaled $\boldsymbol{x} \to h\boldsymbol{x}$.

In the case of uniform conductivity density $K(\boldsymbol{x}) \equiv K$, equation (C11) becomes a regular Poisson equation in two dimensions with dipole source density. The solutions to this equation are well known from the theory of electrostatics, on an infinite domain taking the form

$$\phi(\boldsymbol{x}) = \frac{\boldsymbol{p} \cdot \boldsymbol{x}}{\boldsymbol{x}^2} \tag{C19}$$

$$\boldsymbol{v}(\boldsymbol{x}) = \begin{pmatrix} 0 & 1 \\ -1 & 0 \end{pmatrix} \left(\frac{\boldsymbol{p}}{\boldsymbol{x}^2} - 2\boldsymbol{x}\frac{\boldsymbol{p} \cdot \boldsymbol{x}}{\boldsymbol{x}^4} \right) \tag{C20}$$

for a perturbation at $\boldsymbol{a} = 0$. Indeed, the cycle density decays as $\phi(r) \sim r^{-1}$ and the flow due to the perturbation as $\boldsymbol{v}(r) \sim r^{-2}$.

Appendix D: Relationship between cycle flow and resistance distance

For linear flows, as discussed in IV, the equation (7) governing cycle flows simplifies to

$$Af_c = \kappa q_d \tag{D1}$$

Where

$$L = \left(\begin{array}{c|ccc} L_{11} & L_{12} & L_{13} & \cdots \\ \hline L_{21} & & & \\ L_{31} & & A & \\ L_{41} & & & \end{array} \right)$$

Now, solving (D1) is equivalent to solving the auxiliary equation

$$Lf' = \kappa q'_d \tag{D2}$$

$$f'[1] = 0 \tag{D3}$$

where $q'_d = 0 \otimes q_d$.

(D2) has the solution

$$f' = \kappa L^g q'_d \tag{D4}$$

Where L^g is the Moore-Penrose pseudoinverse of L. Now, Moore-Penrose pseudoinverse is related to the resiatnce distance on a graph by this relation [**?**]

$$L^g_{ij} = -\frac{R_{ij}}{2} + \frac{1}{2|V|}\left(R^{tot}_i + R^{tot}_j\right)$$

Plugging it in (D4), we obtain

$$f_c = \kappa \left(R_{cc_0} - R_{cc_1}\right) + \text{ const}$$